ELECTRON-MICROSCOPIC INVESTIGATION OF A MODULATED (TWEED) STRUCTURE AND OPTICAL CONDUCTIVITY IN ALLOYS AND Y-Ba-Cu-O SINGLE CRYSTALS

E.I. Kuznetsova, L.V. Nomerovannaya, A.A. Mahnev, S.V. Sudareva, I.I. Sasovskaya, I.B. Bobylev, E.P. Romanov

Institute of Metal Physics, Ural Division of RAS, Ekaterinburg, Russia

A correlation between the structure-unstable state of nonstoichiometric $YBa_2Cu_3O_{7-\delta}$ oxides and the loss of metallicity has been established. A comparison with similar states in metal systems is carried out.

Some metallic alloys, such as Ti-Nb, Ti-V, Ni-Al, are known to possess a correlation between optical properties untypical for metals and a specific structure state of these alloys. This state arises before a phase transition either in a critical concentration range, or near it. Thus, for Ti-V alloys the concentrations of 13 - 15 at. % V are the critical ones, and on quenching from 1000 °C the BCC β-phase transforms into ω-phase with atomic displacements from the points of a hexagonal lattice. In that state electron diffraction patterns exhibit not only the reflections of ω-phase, but also an intensive diffuse scattering along the {111}* octahedral planes resulting from atomic displacements.

At some deviation from the critical concentration in Ti-20 at. % Nb alloy an even more intensive diffuse scattering is observed. It has a form of hollow figures inscribed into octahedrons with planes along {111}*, and with intensity maximums in the positions near the nodes of the ω-phase lattice (an incommensurable ω-phase, Fig. 1.). In this case a tweed contrast corresponding to the atom dis-

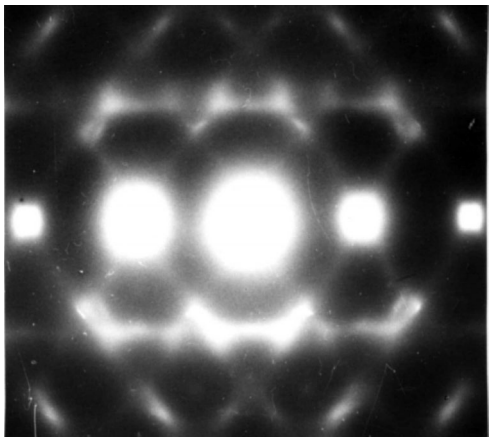

Fig. 1. Electron diffraction pattern of alloy Ti-20 at.% V

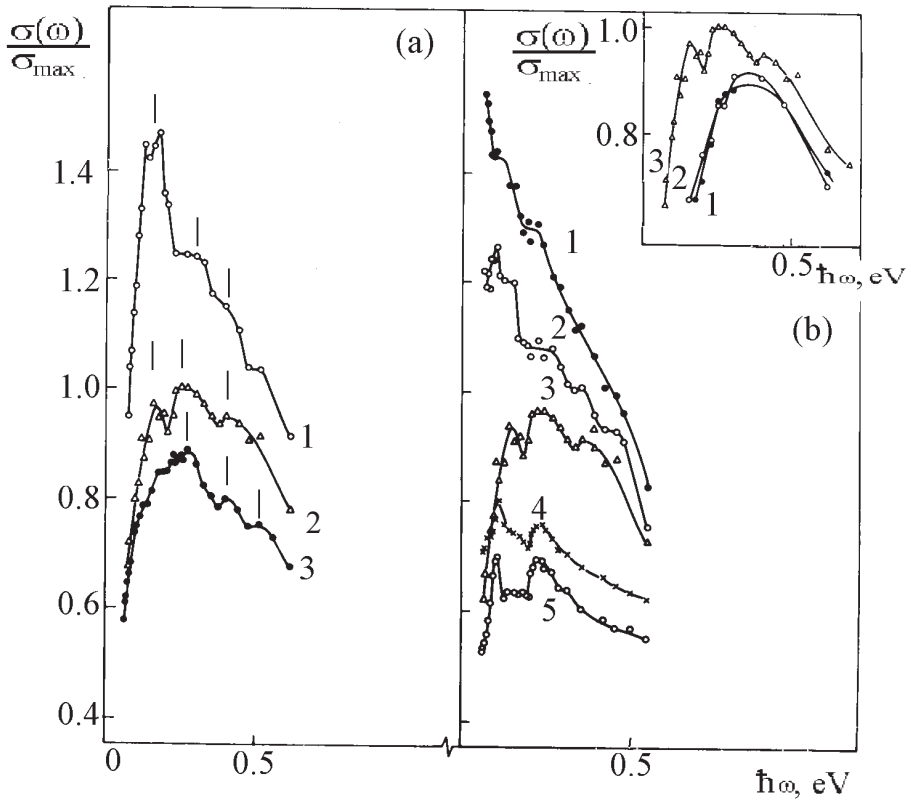

Fig. 2. Optical conductivity of alloys :
a) - Ti-25 at.% Nb (1), Ti-20 at.% V (2), Ti-8 at.%V+4 at.% Mo (3) ; b) - Ti-50 at.% V (1), Ti-30 at.% V (2), Ti-20 at.% V (3), Ti-15 at.% V (4), Ti-13 at.% V (5). Inset shows interband contribution to σ(ω) of Ti alloys with 30 at.% V (1) and 50 at.% V (2) and experimental σ(ω) of alloy Ti-20 at.% V (3)

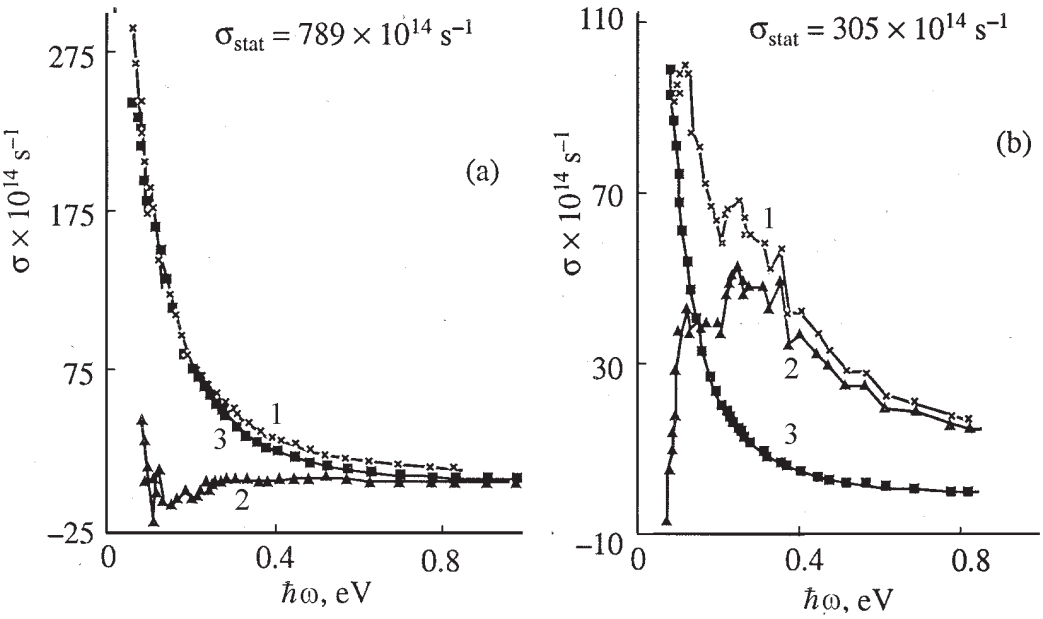

Fig. 3. The dispersion of optical conductivity σ(ω) in Ni-Al alloys with 50 at.% Ni(a), 55 at.% Ni(b): 1-experiment; 2-contribution from interband transitions; 3-calculation by Drude-Ziner equation

placement waves and the space ordering of ω-phase nuclei is observed on micrographs of the structure.

On the σ (ω) plots of Ti alloys with 13, 15, 20 at.% V there are two pronounced singularities: an absorption band with a maximum at 0.25 eV and the absence of a rise from intraband absorption (i.e. the absence of the Drude-Ziner contribution from free carriers) down to energy 0.07 eV (Fig. 2). Nevertheless, the relation $k(\lambda) > n(\lambda)$ indicating the metallic nature of conductivity, is satisfied over the whole investigated infrared (IR) range of the spectrum. Optical conductivity σ(ω) of the Ti alloys with 30 and 50 at.% V has the usual frequency dependence for metals in the IR range [1]. With an increase of vanadium content to 30 at. % the diffuse scattering intensity markedly decreases. The transition from the anomalous optical properties to the normal ones is observed at vanadium content above 20 at. %. It is interesting to note that the alloys can be divided into the same two groups (with anomalous and normal optical properties) according to the sign of the temperature coefficient of resistivity [2], whilst the alloys with a negative coefficient exhibit unusual dispersion of the optical parameters.

An abrupt drop of the square of the plasma frequency is observed on its concentration dependence in the Ti-V alloys with 13-20 at. % V [1]. Thus, the unusual optical properties are found in heterogeneous alloys with unstable structure and ω-regions possessing large atomic displacements and forming a macrolattice in the crystal.

High-frequency conductivity dispersion curves for Ni-Al alloys, as measured in the range 0.07-1.22 eV, are presented in Fig. 3. While the conductivity curve for the alloy with 50 at.% Ni is typical for frequency dependence of metals in the IR region, the σ(ω) of alloys with 55 and 59 at.% Ni has an anomalous behaviour of their optical conductivity: with energy decrease σ(ω) at first increases monotonously, and then such a Drude-like growth is disturbed by a slight fall in a low energy region starting from the energy $h\nu$ = 0.12 eV. As a result, an absorption band is revealed around 0.2 eV [3].

The alloys with 55 and 59 at.% Ni (B2 matrix) are characterized by a planar diffuse scattering on {111}* planes and rather strong rods along <110>* directions which extinguish according to the law for transverse polarized waves and correspond to shear displacements of the {110} planes along the $<1\bar{1}0>$ directions. Electron micrographs reveal a tweed contrast in these alloys, especially strong in the 62.5 at. % Ni-alloy. The electron diffraction patterns of the 62.5 at. % Ni alloy demonstrate the most pronounced effects of the diffuse scattering (Fig. 4).

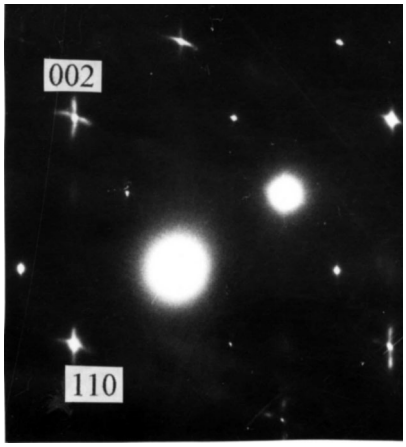

Fig. 4. Electron diffraction pattern of Ni-Al alloy with 62,5 at.% Ni

Now the similar structure and the metallicity loss have been found in the structure-unstable oxides $YBa_2Cu_3O_{7-\delta}$. According to the Khachaturyan and Morris theory [4], the decomposition occurs only in the nonstoichiometric compounds with $\delta > 0.2$, while the oxygen-saturated samples do not decompose. We must verify this experimentally.

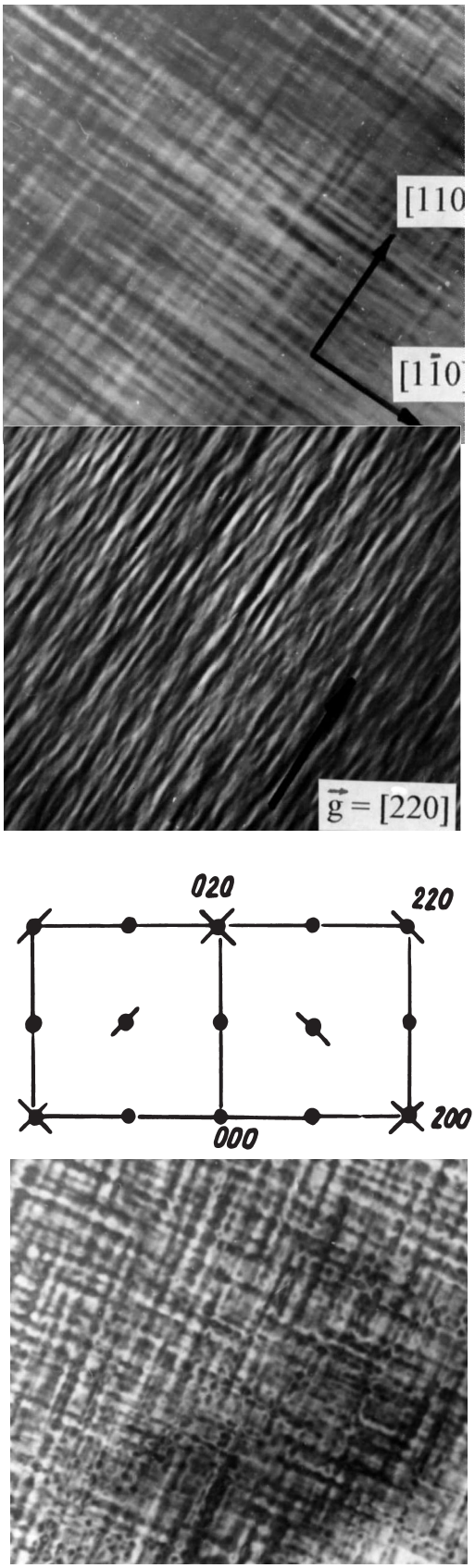

Fig. 5. Structure of a nonstoichiometric $YBa_2Cu_3O_{7-\delta}$ single crystal. Magnification x146000.

(a) bright-field image; $\delta \approx 0.2$; after annealing at 200 °C for 100 h;
(b) dark-field image using 220 reflection;
(c) scheme of an electron diffraction pattern, zone axis [001]; $\delta \approx 0.2$; after annealing at 200 °C for 100 h;
(d) bright field image; $\delta \approx 0.6$; after annealing at 910 °C for 24 h.

Therefore, in the present work we paid special attention to the influence of low- temperature prolonged annealing (at 200 °C for 100 h) on the fine structure and optical properties of nonstoichiometric single crystals.

By electron-microscopy investigation and magnetic susceptibility measurements it has been found that in progressive concentration transition from $YBa_2Cu_3O_7$ to $YBa_2Cu_3O_6$ phase a wide region of structure instability appears, accompanied by the occurrence of periodic and aperiodic waves. The 123 system in the intermediate region of oxygen concentrations is a superposition of two orthorhombic phases with different parameters and oxygen content. The instability of $YBa_2Cu_3O_{6.8}$ compound is found only during a low temperature annealing at 200 °C for 100 h. An early stage of the decomposition with the formation of tweed structure is observed in that case. Besides fine (3-5 nm) precipitates of an oxygen-enriched phase, transversely polarized waves of atomic displacements in the [1$\bar{1}$0] and [110] directions arise in the oxygen-depleted matrix, producing the observed tweed contrast (Fig. 5a). When the diffraction conditions change and the dark-field image is produced in (220) reflection, one of the systems of bands disappears, and the other one is parallel to the $\mathbf{g}_{220}$ vector (Fig. 5b). In the electron-diffraction patterns the diffuse scattering effects are seen as rods along the [110]* directions crossing the nodes of a reciprocal lattice, with extinction typical for transversely polarized waves (Fig. 5c).

In the $YBa_2Cu_3O_{6.4}$ single crystals decomposition into two phases takes place already during cooling from 900 °C because of the smaller stability of the compound with lower oxygen content. A pronounced tweed structure is observed consisting of a grid of orthorhombic phase precipitates and the two systems of transversely polarized atomic displacement waves in the [110] and [1$\bar{1}$0] directions (Fig. 5d).

Optical properties of $YBa_2Cu_3O_{6.8}$ single crystals in an initial state and after a low-temperature annealing at 200°C, 100 h, were investigated in the spectrum range of 0.5 - 5 eV at 290 K. The optical constants $n(\lambda)$ and $k(\lambda)$ of single crystals of the 123 system were measured by the ellipsometric technique. The relative experimental errors for $n(\lambda)$ and $k(\lambda)$ were 2 % - 4 %. The automated ellipsometer for measurements on small samples was assembled on the basis of the KSVU-12 spectrometer.

Optical conductivity spectra $\sigma(\omega)$ of $YBa_2Cu_3O_y$ compounds are already known and described elsewhere [5]. Oxygen depleted specimens with $y = 6{,}1$ are known to have three peculiarities: an absorption peak at 1.7 eV associated with a fundamental edge; a wide band at 2-3 eV and an intensive peak at 4.1 eV. The $\sigma(\omega)$ spectrum of specimens with $y = 6{,}9$ is modified in the following way. A wide band at 2 - 3 eV is retained, the peak at 4.1 eV disappears, and the peak at 1.7 eV is veiled by a contribution of free carriers dominating in the spectrum range of $E < 1.0$ eV. Fig. 6 presents $\sigma(\omega)$ curves of $YBa_2Cu_3O_{6.8}$ specimens before and after the annealing. It should be mentioned that in a spectrum of an initial specimen a weak singularity near 4.0 eV inherent to oxygen depleted specimens has been found. That has been also testified by an absence of a dramatic $\sigma(\omega)$ growth for energies $E < 1$ eV. Radical changes in the

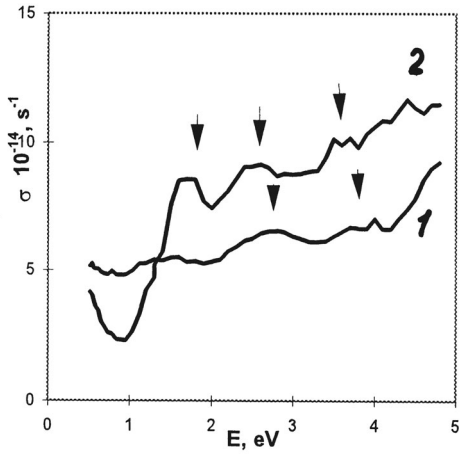

Fig. 6. Optical conductivity σ(ω) of $YBa_2Cu_3O_{6,8}$ before annealing (1) and after annealing (2).

σ(ω) spectra are observed after the annealing. In general the behaviour of σ(ω) differs from that of not annealed specimens both with $y = 6.1$ and with $y = 6.9$. The annealed specimen spectra demonstrate features of both oxygen depleted state and metal state, namely, the sharpening of an absorption edge and a peak at 1.7 eV, along with a presence of an appreciable contribution of free carriers have been observed. Nevertheless, a decrease of free carrier contribution in the annealed state in comparison with the initial one is clearly seen when we analyse a spectrum of a characteristic electron energy losses function. After the annealing a screened plasma frequency $\overline{\omega}_p = \omega_p/\varepsilon_\infty$ (where ω_p is a plasma frequency of current carriers and ε_∞ is a bare dielectric permeability) decreases from 1.65 eV to 1.1 eV.

Thus, the matrix oxygen depletion of the annealed specimen is manifested in a substantial decrease of metallicity and an appearance of a peak at 1.7 eV in the absorption spectrum, typical of specimens with a high oxygen deficiency.

Thus, for a number of different materials a correlation between the structure-unstable state and metallicity loss has been found.

References

1. I.I. Sasovskaya e. a., *Phys. Met. Metall*., **V 65** (1988) 107.
2. A.F. Prekul e. a., *Zh. Eksp. Teor. Fiz*. (Rus), **V 67** (1974) 2286.
3. S.V. Sudareva e. a., *Phys. Met. Metall*., **V 73**, 56 (1992).
4. A.G. Khachaturyan and J.W. Morris, *Phys. Rev. Lett*., **V 59** (1987) 2776.
5. L.V. Nomerovannaya e. a., *Thin Solid Films,* **234** (1993) 531.